Optimization of vehicle-trailer connection systems

2016 J. Phys.: Conf. Ser. 744 012209

(http://iopscience.iop.org/1742-6596/744/1/012209)

Optimization of vehicle-trailer connection systems

F Sorge

DICGIM, Polytechnic School of Palermo University, 90128 – Palermo, Italy

francesco.sorge@unipa.it

Abstract. The three main requirements of a vehicle-trailer connection system are*: en route* stability, over- or under-steering restraint, minimum off-tracking along curved path. Linking the two units by four-bar trapeziums, wider stability margins may be attained in comparison with the conventional pintle-hitch for both instability types, divergent or oscillating. The stability maps are traced applying the Hurwitz method or the direct analysis of the characteristic equation at the instability threshold. Several types of four-bar linkages may be quickly tested, with the drawbars converging towards the trailer or the towing unit. The latter configuration appears preferable in terms of self-stability and may yield high critical speeds by optimising the geometrical and physical properties. Nevertheless, the system stability may be improved in general by additional vibration dampers in parallel with the connection linkage. Moreover, the four-bar connection may produce significant corrections of the under-steering or over-steering behaviour of the vehicle-train after a steering command from the driver. The off-tracking along the curved paths may be also optimized or kept inside prefixed margins of acceptableness. Activating electronic stability systems if necessary, fair results are obtainable for both the steering conduct and the off-tracking.

1. Introduction

It is well known that the lateral dynamics of road vehicles incurs dangerous instability conditions on increasing the running velocity and this trouble gets worse for the multi-unit configuration, where a harder correction task is requested to the driver. The arising instability may be of the divergent type, when the vehicle system swerves from the straight path with an exponential law, or of the oscillating type, when it strays leftwards and rightwards with increasing amplitude.

Extensive researches were made on the influence of the various geometrical and physical characteristics of the vehicle on the anomalous lateral motions. The instability threshold velocity mainly depends on the cornering stiffness of the tyres, which is in turn affected by the vertical load, the inflation pressure, the aspect ratio of the tyre cross section and the ply wrapping.

Besides the instability on the straight paths, also the under- or over-steering trend along the bends must be carefully kept under control, together with the off-tracking of long vehicle systems, when the different paths of the first and last axle may involve the invasion of the opposite direction or the emergency lanes.

All these aspects must be scrupulously faced by the vehicle engineers, particularly for the long and heavy vehicles. The best solution to limit all possible drawbacks is always difficult to pursue and one has to weigh up advantages and disadvantages of the most promising configurations of the tow arrangement. In this connection, suitable electronic stability programs (ESP) may help in limiting the anomalous steering response [1], and proper hydraulic dampers may contrast the instability behaviour

of the vehicle at the highest speeds. ESP systems may be of various types: differential braking systems which apply differential braking to the left and right wheels; steer-by-wire systems which correct the steering angle automatically; active torque distribution systems which also control the drive torque.

All the above anomalous motions are strongly influenced by the tyre transverse deformation and the cornering trend of the wheel run, which phenomenon received much attention in the past.

Rocard was perhaps the first who gave a theoretical description of the vehicle lateral dynamics [2]. He studied the interdependence between the drift angle of the wheel and the transverse reaction force applied by the road through the ground print: this reaction force increases on increasing the vertical load on the tyre, at least beneath a certain load level. Gillespie reports many experimental results in the chapter on the steady-state cornering of his treatise on vehicle dynamics, highlighting the influence of various geometrical and physical characteristics of the tyres, such as the inflation pressure, which increases the cornering stiffness, or the tyre aspect ratio, which reduces it [3]. The most complete formulation for the correlation between the cornering force and the wheel slip angle has been probably proposed by Pacejka [4]. It was named by the author the "magic formula" and contains several parameters that may be properly adjusted to fit all types of tyre response.

The last decades report many other researches on these subjects. As a few examples, we recall some of them: Fratila and Darling [5], who use a 24 degrees of freedom model to investigate the abnormal motions of a vehicle-caravan system; Rossetter and Gerdes [6], who treat the yaw stabilization of a single vehicle by control systems combining differential braking and steering; Hac *et al.* [7], who study the active braking of a vehicle-trailer train. The lateral stability of multi-trailer trucks was examined in the eighties applying several connection arrangements, including articulated linkages, and some of them revealed interesting stabilizing properties (see [8]). Many devices were also patented and some types are present in the market [9].

The promising properties of the articulated connection between tractors and semi-trailers in terms of stability are the starting point of the present analysis, where a four-bar linkage is considered in place the single pintle-hitch. The self-feeding lateral motions along the straight paths are examined and the response to the steering manoeuvres of the driver are quantified. The aim is to create a simple model for the search of the instability thresholds of the vehicle speed, and for the check of the criticality of the vehicle-trailer path along the bends. The aid from the possible active control of the steering behaviour is also taken into account for some configurations.

The author has recently proposed an articulated connection arrangement of the Roberts' four-bar type [10]. Here, enlarging the range of the possible configurations, a more general approach is addressed to the optimization of the connection systems in terms of run stability and steering conduct. Assuming small lateral movements, the model is linearized, so that the stability thresholds are searched by the analysis of the characteristic roots and the response to the steering commands is calculated by solving linear algebraic systems.

2. Theoretical model

2.1. Scheme and deformation of the tow connection

It is assumed that the lateral movements of the car train are of small amplitude.

The tow system is schematized in figure 1, where

- the frames Oxy and $G_l\xi\eta$ are fixed to the ground and to the leading unit respectively;
- θ_l and θ_t are the angles formed by the leading and trailing units with the fixed direction y, whence the relative rotation is defined as $\theta_{lt} = \theta_l - \theta_t$;
- G_l and G_t are the centres of mass of the leading and trailing units;
- $F_{b\xi}$ and $F_{b\eta}$ are the components along ξ and η of the resultant traction force acting on the semi-trailer through the two connecting bars, which may be applied at the instant centre I of the relative rotation;
- $F_{d\xi}$ and $F_{d\eta}$ are the components along ξ and η of the resultant force exerted on the semi-trailer by the two dampers, which may be applied at the intersection D of their axes;

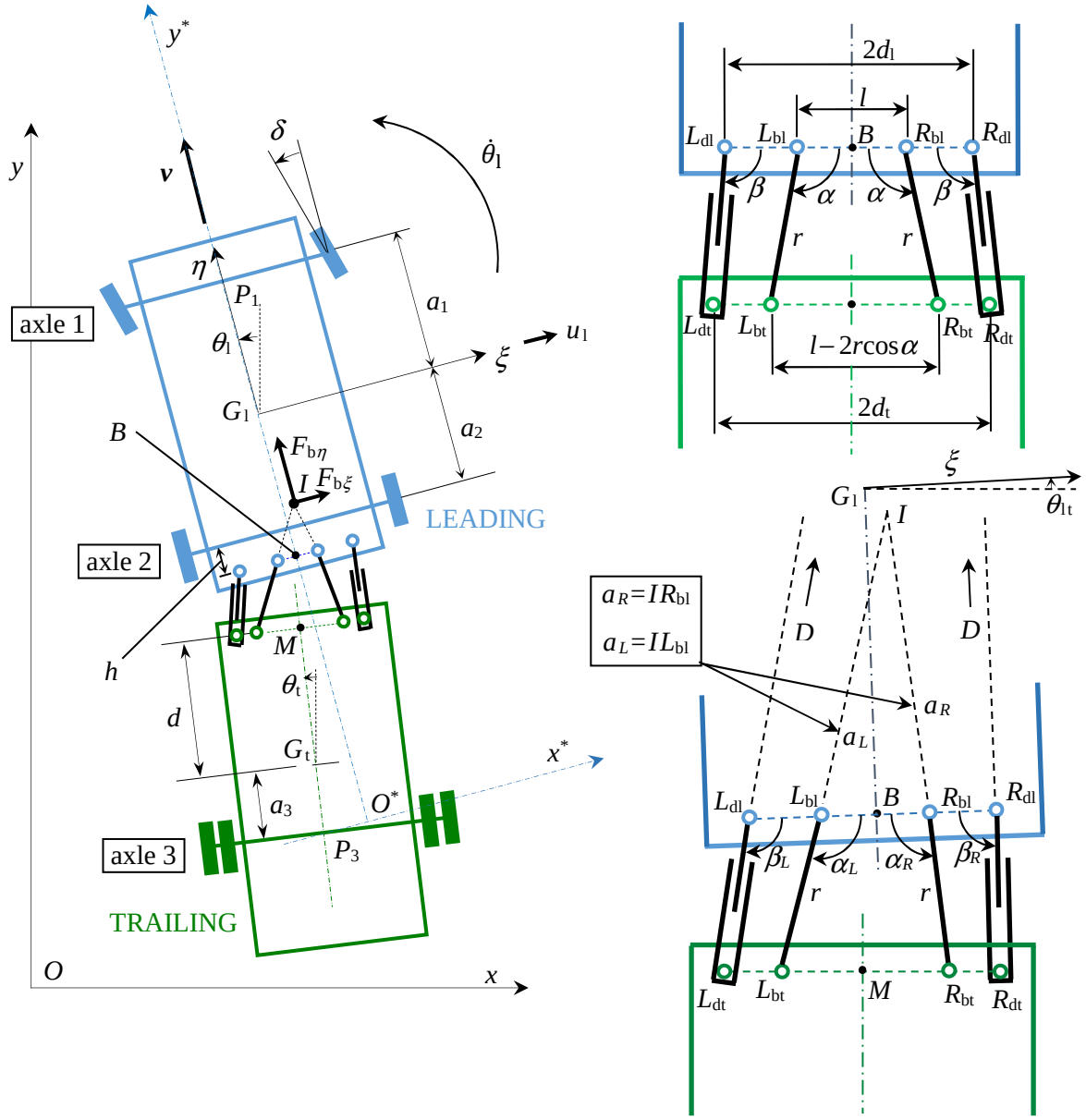

Figure 1. Scheme of the two-unit system and of the articulated connection. On the right, details of the connection in the non-deformed and deformed configurations (up and down respectively).

- δ is the steering angle imposed by the driver, which is assumed of the same small order of magnitude of the yaw rotation and equal for the left and right wheels for simplicity;
- v is the vehicle speed.

Both traction and damping quadrilaterals, $L_{bl}R_{bl}R_{bt}L_{bt}$ and $L_{dl}R_{dl}R_{dt}L_{dt}$, are isosceles trapeziums in the central configuration. Three types of connection arrangement are classifiable: with backward converging, inter-crossing and forward converging side bars $L_{bl}L_{bt}$ and $R_{bl}R_{bt}$. For all arrangements, the following closure equations hold (see figure 1)

$$r\cos\alpha_L + (l - 2r\cos\alpha)\cos\theta_{lt} + r\cos\alpha_R = l$$
$$r\sin\alpha_L + (l - 2r\cos\alpha)\sin\theta_{lt} - r\sin\alpha_R = 0 \qquad (1a,b)$$

and similar closure conditions apply to the triangle $L_{bl}IR_{bl}$

$$a_L\cos\alpha_L + a_R\cos\alpha_R = l\,\mathrm{sgn}(\cos\alpha)$$
$$a_L\sin\alpha_L - a_R\sin\alpha_R = 0 \qquad (2a,b)$$

Putting $\Delta\alpha_L = \alpha_L - \alpha$, $\Delta\alpha_R = \alpha_R - \alpha$, and considering small lateral movements, i. e. $|\Delta\alpha_L| << \alpha$, $|\Delta\alpha_R| << \alpha$, the incremental angles $\Delta\alpha_L$, $\Delta\alpha_R$ and $\theta_l - \theta_t = \theta_{lt}$ are of the same small order of magnitude, which is also assumed ascribable to the cornering slip angles ε. Thus, ignoring all nonlinear terms, i. e. of order ε^2 or smaller, and proceeding as in [10], one gets by (1-2):

$$\Delta\alpha_L \cong -\Delta\alpha_R \cong \theta_{lt}\left(1 - \frac{l}{2r\cos\alpha}\right) \qquad (3)$$

$$a_L \cong \frac{l\,\mathrm{sgn}(\cos\alpha)}{\sin 2\alpha}(\sin\alpha - \Delta\alpha_L\cos\alpha) \qquad a_R \cong \frac{l\,\mathrm{sgn}(\cos\alpha)}{\sin 2\alpha}(\sin\alpha - \Delta\alpha_R\cos\alpha) \qquad (4a,b)$$

These results yield the linearized coordinates ξ, η of points I and M.

$$\xi_I \cong \frac{l\theta_{lt}}{\sin 2\alpha}\left(\frac{l}{2r\cos\alpha} - 1\right) \qquad \eta_I \cong -\left(\frac{l\tan\alpha}{2} + a_2 + h\right)$$
$$\xi_M \cong r\sin\alpha\,\theta_{lt}\left(\frac{l}{2r\cos\alpha} - 1\right) \qquad \eta_M \cong -(r\sin\alpha + a_2 + h) \qquad (5a,b,c,d)$$

The maximum relative rotation between the trailer and the tractor depends on the connection arrangement and is an important parameter concerning the manoeuvrability in small spaces. For backward converging bars, the relative rotation is maximum when the trailer side is aligned with one of the two drawbars. This angle is not so large (quite less than 90°) and this might be a drawback of this scheme. Putting $\alpha_L = \theta_{lt,max.}$ into Equations (1a,b), solving with respect to $r\cos\alpha_R$ and $r\sin\alpha_R$, squaring and summing, one gets:

$$\theta_{lt,max.,backw.} = \cos^{-1}\left[\frac{l^2+(r+l-2r\cos\alpha)^2-r^2}{2l(r+l-2r\cos\alpha)}\right] \qquad \text{(backward trapezium)} \qquad (6)$$

In the case of inter-crossing bars, $l - 2r\cos\alpha$ is negative and we must distinguish. If $2r\cos\alpha - l > l$, we have a double-crank mechanism by the Grashof's rule and a complete relative rotation of 360° may be covered by the trailer with respect to the tractor, similarly to the conventional pintle-hitch. If $2r\cos\alpha - l < l$, the maximum relative rotation is reached when the trailer side, after passing from the first alignment position with one drawbar, keeps on rotating until it is aligned with the other bar. The value of $\theta_{lt,max.,cross.}$ is similar to Equation (6), save that $r + l - 2r\cos\alpha$ is replaced by $-r + l - 2r\cos\alpha$, and is much larger (more than 90°). For the forward converging bars, the maximum rotation occurs when the instant centre I runs to infinite, i. e. when the two side bars are parallel and $\alpha_L = 2\pi - \alpha_R$. Using Equations (1a,b), eliminating the angles α_L and α_R by squaring and summing, one gets

$$\theta_{lt,max.,forw.} = \cos^{-1}\left[\frac{l^2+(l-2r\cos\alpha)^2-4r^2}{2l(l-2r\cos\alpha)}\right] \qquad \text{(forward trapezium)} \qquad (7)$$

and angles close to 90° may be reached.

For small displacements, the paths of the points belonging to the longitudinal axes of symmetry in the relative motions of the trailer with respect to the tractor or vice versa, and particularly the paths of the inflexion poles, are nearly straight and orthogonal to the axes. This property simplifies the realization of the support track of the "fifth wheel" in the connection assembly.

The coordinates ξ and η of points L_{dl}, R_{dl}, L_{dt} and R_{dt} are given by

$$\xi_{R_{dl}\text{or}L_{dl}} = \pm d_l \ \ (+\text{ for } R_{dl} \text{ and } -\text{for } L_{dl}) \qquad \xi_{R\text{dt or }L\text{dt}} = \xi_M \pm d_t\cos\theta_{vt} \ \ (+\text{ for } R_{dt} \text{ and } -\text{for } L_{dt})$$
$$\eta_{R_{dl}\text{or}L_{dl}} = -h - a_2 \qquad \eta_{L\text{dt or }R\text{dt}} = \eta_M \pm d_t\sin\theta_{vt} \ \ (+\text{ for } L_{dt} \text{ and } -\text{for } R_{dt}) \qquad (8a,b,c,d)$$

and using Equations (5c,d) and (8), one gets the approximate projections of the lengths of the two dampers along ξ and η, and then the lengths and the inclination angles β:

$$l_{R_\mathrm{d}\mathrm{or}L_\mathrm{d}} \cong \sqrt{(d_\mathrm{t}-d_\mathrm{l})^2+(r\sin\alpha)^2}\left[1 \pm \frac{(d_\mathrm{t}-d_\mathrm{l})\left(\frac{l}{2r\cos\alpha}-1\right)+d_\mathrm{t}}{(d_\mathrm{t}-d_\mathrm{l})^2+(r\sin\alpha)^2}\, r\sin\alpha\,\theta_\mathrm{lt}\right]$$

$$\tan\beta_{R_\mathrm{d}\mathrm{or}L_\mathrm{d}} \cong -\frac{r\sin\alpha}{d_\mathrm{t}-d_\mathrm{l}} \pm \left[\left(\frac{l}{2r\cos\alpha}-1\right)\left(\frac{r\sin\alpha}{d_\mathrm{t}-d_\mathrm{l}}\right)^2-\frac{d_\mathrm{t}}{d_\mathrm{t}-d_\mathrm{l}}\right]\theta_\mathrm{lt} \qquad (9a,b,c)$$

$$\Delta\beta_{R_\mathrm{d}\mathrm{or}L_\mathrm{d}} = \beta_{R_\mathrm{d}\mathrm{or}L_\mathrm{d}} - \beta = \beta_{R_\mathrm{d}\mathrm{or}L_\mathrm{d}} + \tan^{-1}\left(\frac{r\sin\alpha}{d_\mathrm{t}-d_\mathrm{l}}\right)$$
$$\cong \pm\cos^2\beta\left[\left(\frac{l}{2r\cos\alpha}-1\right)\left(\frac{r\sin\alpha}{d_\mathrm{t}-d_\mathrm{l}}\right)^2-\frac{d_\mathrm{t}}{d_\mathrm{t}-d_\mathrm{l}}\right]\theta_\mathrm{lt}$$

Here, the plus or minus signs refer to the right (R_d) or left (L_d) damper. The forces exerted by the dampers on the trailer may be obtained multiplying their damping coefficient c_v by the sliding velocities, $\dot{l}_{R_\mathrm{d}}$ or $\dot{l}_{L_\mathrm{d}}$. The components of the resultant force along ξ and η, are applicable at point D and turn out to be, saving only first order terms and indicating the time derivatives with dots:

$$F_{\mathrm{d}\xi} \cong c_v\cos\beta\left(\dot{l}_{R_\mathrm{d}}-\dot{l}_{L_\mathrm{d}}\right) \cong 2c_v\cos\beta\,\frac{(d_\mathrm{t}-d_\mathrm{l})\left(\frac{l}{2r\cos\alpha}-1\right)+d_\mathrm{t}}{\sqrt{(d_\mathrm{t}-d_\mathrm{l})^2+(r\sin\alpha)^2}}\, r\sin\alpha\,\dot{\theta}_\mathrm{lt} \qquad (10a,b)$$

$$F_{\mathrm{d}\eta} \cong c_v\sin\beta\left(\dot{l}_{R_\mathrm{d}}+\dot{l}_{L_\mathrm{d}}\right) \cong 0$$

The coordinates of the intersection point D of the damper axes may be calculated like the ones of I, replacing a with b, α with β, l with $2d_\mathrm{l}$ into Equations (2) and using Equations (9c)

$$\xi_D \cong d_\mathrm{l}\theta_\mathrm{lt}\left[\left(\frac{l}{2r\cos\alpha}-1\right)\left(\frac{r\sin\alpha}{d_\mathrm{t}-d_\mathrm{l}}\right)-\frac{d_\mathrm{t}}{r\sin\alpha}\right] \qquad \eta_D \cong -(d_\mathrm{l}\tan\beta + a_2 + h) \qquad (11a,b)$$

The distances of D from the mass centres G_l and G_t in the non-deformed configuration are $|\eta_D|$ and $|d + r\sin\alpha - d_\mathrm{l}\tan\beta|$ respectively. Yet, these distances may be also used for the approximate calculation of the damping moments on the two units during the sway motion.

If $d_\mathrm{t} = d_\mathrm{l}$ and $\beta = 90°$, then $l_{R_\mathrm{d}\mathrm{or}L_\mathrm{d}} \cong r\sin\alpha \pm d_\mathrm{t}\theta_\mathrm{lt}$ by (9a), but the approximate expressions (9b,c) become indeterminate and no longer hold. Using the complementary angles $\beta_\mathrm{c} = 90° - \beta$, it is possible to find that $\Delta\beta_{\mathrm{c},R_\mathrm{d}\mathrm{or}L_\mathrm{d}} \to \pm[1 - l/(2r\cos\alpha)]\theta_\mathrm{lt}$ for $\beta_\mathrm{c} \to 0°$. The dampers remain nearly parallel and the damping moments on the trailer and the tractor are $\pm 2c_v d_\mathrm{t}^2\dot{\theta}_\mathrm{lt}$.

At last, notice that the force $F_{\mathrm{b}\eta}$ applied at point I is approximately the resistant road force acting on the trailer and is equal in practice to the air drag for non-negligible velocities, whence one may put $F_{\mathrm{b}\eta} = F_{\mathrm{air,trailer}} = ½\,(c_x\rho A v^2)$.

2.2. Tyre cornering and equations of motion

The transverse force exerted by the ground orthogonally to the wheel depends on several working conditions and may be roughly considered proportional to the slip angle, $F \cong -k\varepsilon$ [2]. Several formulas and experimental data were proposed to consider the various working conditions of the wheel. For example, the diagram of figure 10.15 from reference [3] shows the trend of the cornering stiffness k on increasing the vertical load on the tyre (% of rated load). Expressing ε in radians, an excellent fit with this diagram was here found by a third degree parabolic law:

$$k = -\frac{F}{\varepsilon} = a + b\left(\frac{F_z}{F_{z0}}\right) - c\left(\frac{F_z}{F_{z0}}\right)^3 \qquad \text{where} \qquad (12a,b)$$

a = 5.092 kN b = 39.735 kN c = 6.955 kN

These values will be used in the following and it is also planned that *a*, *b* and *c* may be multiplied by a common factor g_3 for the wheels of the trailer axle, in order to take into account possible differences of the inflation pressure, or the ply composition, or the tyre aspect ratio.

The slip angle is given by the ratio of the components of the wheel centre velocity along the directions orthogonal and parallel to the rim plane. In practice, the former is equal to the lateral slip velocity at the ground print and the latter to the vehicle velocity *v*. The slip velocities on the one and the other side of each axle are both equal to the yaw velocity of the axle midpoint (bicycle model).

Indicating the component of the velocity of G_l along ξ with u_l, the component $\dot{x}_{G_l}$ along *x* is given by $\dot{x}_{G_l} = u_l - v\theta_l$ and the slip velocities of the wheels on the axles 1 and 2 are

$$u_l - a_1\dot{\theta}_l + v\delta \ \text{(front axle)} \qquad u_l + a_2\dot{\theta}_l \ \text{(rear axle)} \qquad (13a,b)$$

where the steering angle δ was considered in the front axle 1.

The slip velocity of the wheels of the trailer axle 3 is given by the sum of the transverse velocities of the instant centre *I* and of the axle midpoint with respect to *I*. According to figure 1, one gets

$$u_l - \eta_I\dot{\theta}_l + \left(\eta_I - \eta_{G_t} + a_3\right)\dot{\theta}_t - v\theta_{lt} \quad \text{(trailer axle)} \qquad (14)$$

where $\eta_I - \eta_{G_t} \cong d + r\sin\alpha - l\tan\alpha/2$.

Hence, the slip angles are

$$\varepsilon_1 = \frac{u_l - a_1\dot{\theta}_l}{v} + \delta \qquad \varepsilon_2 = \frac{u_l + a_2\dot{\theta}_l}{v}$$
$$\varepsilon_3 = \frac{u_l + \left(a_2 + h + \frac{l}{2}\tan\alpha\right)\dot{\theta}_l + \left(d + r\sin\alpha - \frac{l\tan\alpha}{2} + a_3\right)\dot{\theta}_t}{v} - \theta_{lt} \qquad (15a,b,c)$$

The equilibrium conditions on the vertical plane permits calculating the vertical loads F_{zi} on the wheels. The cornering forces oppose the lateral slip and may be written in the form:

$$F_i = -2n_i g_i k_i \varepsilon_i = -2n_i g_i\left[a + b\left(\frac{F_{zi}}{F_{zi0}}\right) - c\left(\frac{F_{zi}}{F_{zi0}}\right)^m\right]\varepsilon_i \qquad (16)$$

for each axle *i* (= 1, 2, 3), where n_i indicates the number of wheel pairs of that axle. It is supposed that $n_i = g_i = 1$ for $i = 1$ and 2, that the rated loads F_{zi0} correspond to the trailer self-balance ($a_3 = 0$) and that the thrust block is located at *B* (see figure 1).

The sway motion may be just described by three state variables, u_l, $\dot{\theta}_l$ and θ_{lt}, but four dynamical equations must be formulated in total for the two units, two translational ones along *x* and two rotational ones. Nevertheless, one equation drops when eliminating the unknown force $F_{b\xi}$ applied at *I*.

Using Equations (5a,b), we get

$$(m_l + m_t)\left(\dot{u}_l - v\dot{\theta}_l\right) + m_t\left(a_2 + h + \frac{l}{2}\tan\alpha\right)\ddot{\theta}_l + m_t\left(d + r\sin\alpha - \frac{l\tan\alpha}{2}\right)\left(\ddot{\theta}_l - \ddot{\theta}_{lt}\right)$$
$$+2k_1\varepsilon_1 + 2k_2\varepsilon_2 + 2k_3n_3g_3\varepsilon_3 + F_{\text{air,trailer}}\theta_{lt} = 0 \qquad (17a,b,c)$$
$$m_l\rho_l^2\ddot{\theta}_l + 2k_2a_2\varepsilon_2 - 2k_1a_1\varepsilon_1 - \left(a_2 + h + \frac{l}{2}\tan\alpha\right)\left[m_l\left(\dot{u}_l - v\dot{\theta}_l\right) + 2k_1\varepsilon_1 + 2k_2\varepsilon_2\right]$$
$$+ F_{\text{air,trailer}}\frac{l}{\sin 2\alpha}\left(\frac{l}{2r\cos\alpha} - 1\right)\theta_{lt}$$

$$+2c_v\cos\beta\,\frac{(d_t-d_l)\left(\frac{l}{2r\cos\alpha}-1\right)+d_t}{\sqrt{(d_t-d_l)^2+(r\sin\alpha)^2}}\,(d_l\tan\beta+a_2+h)r\sin\alpha\,\dot{\theta}_{lt}=m_{ESP}$$

$$m_t\rho_t^2\left(\ddot{\theta}_l-\ddot{\theta}_{lt}\right)-\left(d+r\sin\alpha-\frac{l\tan\alpha}{2}\right)\left[m_l\left(\dot{u}_l-v\dot{\theta}_l\right)+2k_1\varepsilon_1+2k_2\varepsilon_2\right]+2k_3n_3g_3a_3\varepsilon_3$$
$$-F_{air,trailer}\left[d+r\sin\alpha-\frac{l\tan\alpha}{2}+\frac{l}{\sin 2\alpha}\left(\frac{l}{2r\cos\alpha}-1\right)\right]\theta_{lt}$$

$$+2c_v\cos\beta\,\frac{(d_t-d_l)\left(\frac{l}{2r\cos\alpha}-1\right)+d_t}{\sqrt{(d_t-d_l)^2+(r\sin\alpha)^2}}(d\ +r\sin\alpha-d_l\tan\beta)r\sin\alpha\,\dot{\theta}_{lt}=0$$

where ρ_l and ρ_t are the radii of gyration of the vehicle and the trailer and m_{ESP} indicates the correction moment exerted on the leading unit by some possible ESP system. Notice that Equation (17a) expresses the transverse dynamical equilibrium of the whole two-unit vehicle, where the term $-v\dot{\theta}_l(m_l + m_t)$ is in practice the total centrifugal force, and that the trinomial $\left[m_l\left(\dot{u}_l-v\dot{\theta}_l\right)+2k_1\varepsilon_1+2k_2\varepsilon_2\right]$ represents the mutual transverse force $F_{b\xi}$.

The state equations may be turned into non-dimensional form. Introducing the reference cornering stiffness $k_0 = a + b - c$ and the reference speed $v_0=\sqrt{k_0a_1/m_l}$, define the dimensionless parameters:

$A_i = a_i / a_1$	ratio of axle distances
$c_0 = F_{air,trailer}/(k_0V^2)$	aerodynamic coefficient
$C_v = c_v v_0 / k_0$	damping coefficient
$K_i = n_i g_i k_i / k_0$	cornering stiffness
$H_l = (a_2 + h + l\tan\alpha/2)/a_1$	distance between G_l and I
$H_t = (d + r\sin\alpha - l\tan\alpha/2)/a_1$	distance between I and G_t
$L=\frac{l}{a_1\sin 2\alpha}\left(\frac{l}{2r\cos\alpha}-1\right)=\xi_I/(a_1\theta_{vt})$	coefficient of displacement of point I from mid plane
$M_{ESP} = m_{ESP}/(2a_1k_1\delta)$	ESP correction moment
$U = u_l/v_0$	transverse velocity of vehicle centre
$V = v/v_0$	speed
$\mu = m_t/m_l$	mass ratio
$P_l = \rho_l/a_1$, $P_t = \rho_t/a_1$	radii of gyration of vehicle and trailer
$\tau = v_0t/a_1$	time variable
$\Omega = a_1\dot{\theta}_l/v_0$	angular velocity of vehicle

Defining the differential operator $D^{(j)}(...) = d^j(...)/d\tau^j = (a_1/v_0)^j\, d^j(...)/dt^j$, dividing Equation (17a) by k_0 and Equations (17b,c) by k_0a_1, the differential system changes into

$$[D]\times\{U\quad\Omega\quad\theta_{lt}\}^T=2K_1\delta\{-1\quad(1+H_l+M_{ESP})\quad H_t\}^T \tag{18a,b}$$

where the dynamic matrix [D] is given by:

$$\begin{bmatrix} (1+\mu)D^{(1)} + \frac{2(K_1+K_2+K_3)}{V}D^{(0)} & \mu(H_\mathrm{l}+H_\mathrm{t})D^{(1)} + \frac{2[K_2A_2-K_1+K_3(H_\mathrm{l}+H_\mathrm{t}+A_3)]-(1+\mu)V^2}{V}D^{(0)} & -\mu H_\mathrm{t}D^{(2)} - \frac{2K_3(H_\mathrm{t}+A_3)}{V}D^{(1)} + (c_0V^2-2K_3)D^{(0)} \\ -H_\mathrm{l}D^{(1)} + \frac{2[K_2A_2-K_1-H_\mathrm{l}(K_1+K_2)]}{V}D^{(0)} & P_\mathrm{l}^2D^{(1)} + \frac{2[K_2A_2^2+K_1-H_\mathrm{l}(K_2A_2-K_1)]+H_\mathrm{l}V^2}{V}D^{(0)} & C_vD_\mathrm{l}D^{(1)} + Lc_0V^2D^{(0)} \\ -H_\mathrm{t}D^{(1)} + \frac{2[K_3A_3-H_\mathrm{t}(K_1+K_2)]}{V}D^{(0)} & \mu P_\mathrm{t}^2D^{(1)} + \frac{2[K_3A_3(H_\mathrm{l}+H_\mathrm{t}+A_3)-H_\mathrm{t}(K_2A_2-K_1)]+H_\mathrm{t}V^2}{V}D^{(0)} & -\mu P_\mathrm{t}^2D^{(2)} - \left[\frac{2K_3A_3(H_\mathrm{t}+A_3)}{V}-C_vD_\mathrm{t}\right]D^{(1)} - [c_0V^2(L+H_\mathrm{t})+2K_3A_3]D^{(0)} \end{bmatrix}$$

The factors D_v and D_t in the third column stem from the last addends of Equations (17b,c), leaving out c_v and $\dot{\theta}_{\mathrm{vt}}$ and dividing by a_1^2. For parallel dampers ($\beta = 90°$), one gets $D_\mathrm{l} = -D_\mathrm{t} = 2(b_\mathrm{t}/a_1)^2$.

3. Stability and steering response of articulated vehicles

3.1. Stability

The homogeneous solution of Equation (18a) may be obtained equating to zero the right hand and replacing the operators $D^{(j)}$ with the j^{th} powers of the characteristic number λ. We get a fourth degree algebraic equation, whose coefficients c_i are functions of the car velocity,

$$\lambda^4 + c_1\lambda^3 + c_2\lambda^2 + c_3\lambda + c_4 = 0 \tag{19}$$

The roots must have negative real part for stability.

The divergent instability threshold is determined equating c_4 to zero, whereas the oscillating instability threshold may be obtained putting $\lambda = \pm i\omega$ and equating the real and imaginary parts of the characteristic equation to zero separately:

$$\begin{array}{llll} \omega^4 - c_2\omega^2 + c_4 = 0 & \pm i\omega(c_3 - c_1\omega^2) = 0 & & \text{whence} \\ \omega^2 = \frac{c_3}{c_1} & \text{and} & c_3^2 - c_1c_2c_3 + c_1^2c_4 = 0 & \text{(provided that } c_3/c_1 > 0\text{)} \end{array} \tag{20}$$

It is noteworthy that the condition $c_3 = 0$ implies two complex roots with zero imaginary parts, which corresponds to a bifurcation point on the real axis of the root locus on the Argand-Gauss plane. The Hurwitz method is then used to check the stable or unstable nature of a few sample points in the regions bounded by the threshold curves.

A great deal of connection configurations may be quickly checked and stability maps may be traced for the instability thresholds, where for example one may choose the dimensionless distances A_3 of the trailer axle from the mass centre as ordinates, and the dimensionless velocities V as abscissae. The range of A_3 must not be too large, to avoid an excessive load on the thrust box (this load is zero for $A_3 = 0$), whereas the range of $V = v/v_0$ is chosen between 0 and 10, which is quite wide as the usual values of k_0, a_1 and m_l give $v_0 \cong 6$ m/s (20-24 km/h). The other parameters of the articulated vehicle are held fixed in the stability search and it is assumed that $\mu = 1$ and two pairs of wheels are mounted on the third axle ($n_3 = 2$) for a well-balanced load distribution.

As will be shown in the next subsection, a correct path of the articulated vehicle along a bend requires rather stiff cornering coefficients on the third axle. Therefore, it will be assumed that the trailer wheels may have larger sizes and higher inflation pressure than the tractor, which may be handled in the analysis by properly choosing a common multiplicative factor g_3 for the coefficients a, b and c of Equation (12).

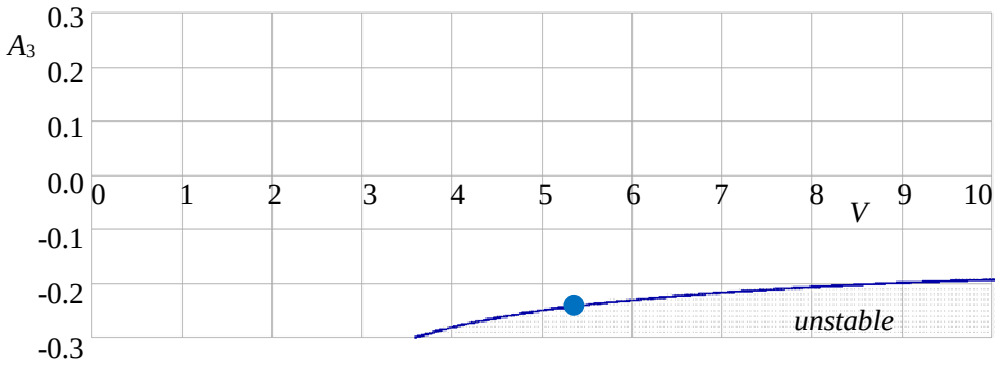

Figure 2. Threshold of oscillating instability for a four-bar linkage with forward converging bars. Third axle offset vs. vehicle velocity.

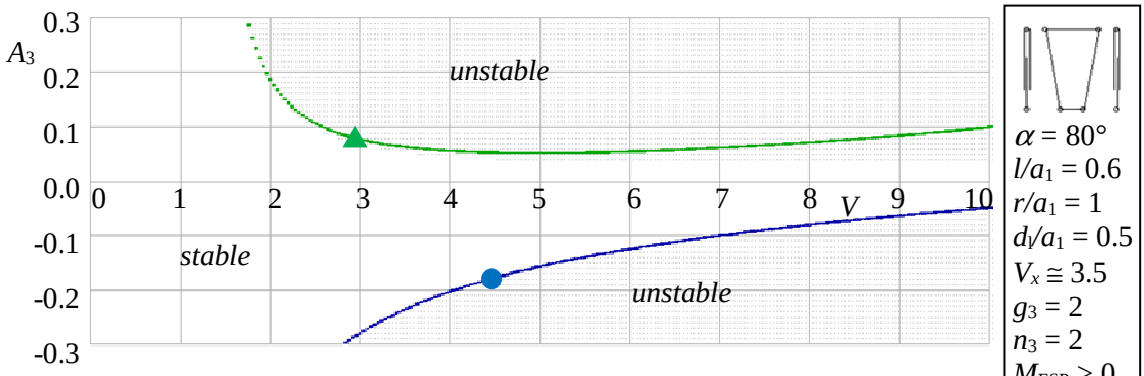

Figure 3. Threshold of instability for a four-bar linkage with backward converging bars. Third axle offset vs. vehicle velocity. Circles: oscillating instability thresholds. Triangles: divergent instability thresholds.

Figures 2 and 3 show the stability maps for two example cases, which were chosen in the group of the most promising ones in terms of correct response along the bends and refer to forward and backward converging drawbars respectively. The unstable regions are indicated with darkened colouring, together with those region that, even though stable, lie on the right of unstable regions, which must be necessarily crossed on increasing the speed. The circles and triangles refer to oscillating and exponential instability thresholds respectively. The forward converging connection proves to be more stable in general and the action of the dampers is not needed (figure 2). On the contrary, the backward one would exhibit much larger instability regions without dampers, which become then necessary to get acceptable stability. The use of dampers might appear as an unavoidable drawback of the backward connection, because their reaction forces are of the same order of magnitude as the cornering forces on the wheels and one could be inclined to expect some increase of the transient times following the steering commands from the drivers. Nevertheless, imposing step δ–inputs and velocities of full stability, the numerical solutions of the full equations (18a) by a fourth-order Runge-Kutta routine indicates settling times that are only slightly longer than the non-damped systems, both being of the order of 1 s roughly. In return, the backward connection may yield positions of the instant centre I that are very close to the mass centre of the trailer, which is very beneficial as regards the reduction of the off-tracking, as will be shown later.

Equations (20) also yield the frequency of the arising oscillating instability. As the real eigenvalues in the time domain are obtainable multiplying λ and ω by v_0/a_1 and the dimensionless angular frequencies ω are considerably lower than one, the path wavelength turns out to be much greater than the length of the whole car train.

3.2. Steering response

The steady response of the articulated vehicle to a steering manoeuvre operated by the driver may be calculated cancelling all operators $D^{(i)}$ for $i > 0$ in Equations (18), including the right hands, all proportional to δ, and solving for the ratios U/δ, Ω/δ and θ_{lt}/δ. On increasing V, the solution of the complete system is stopped when reaching the instability threshold, which occurs with asymptotes or abruptly at finite points for the divergent or oscillating instability thresholds respectively. Ignoring M_{ESP}, the relative rotation θ_{lt} is finite for $v \to 0$, because the determinant $\det(D_{steady})$ of the steady dynamical matrix and all cofactors of its third column are of order $1/V^2$, but U and Ω tend to zero.

After solving the complete system, the radius of curvature ρ of the tractor path can be calculated and compared with the ideal radius in the absence of under- and over-steering, $\rho_{id.} \cong (a_1 + a_2)/\delta$.

$$\rho = \frac{v}{\dot{\theta}_l} = \frac{V a_1}{\theta'_l} \qquad \rightarrow \qquad \frac{\rho}{\rho_{id.}} = \frac{V\delta}{\Omega(1 + A_2)} \tag{21a,b}$$

Moreover, it is possible to characterize the off-tracking behaviour of the car train by the difference between the path radii of the mid-points P_1 and P_3 of the first and third axles, assuming steady running along a road bend. Assigning the initial time ($t = 0$) to some arbitrary position of the vehicle, it is possible to fix a new reference frame $O^*x^*y^*$ whose x^* axis contains P_3 and whose y^* axis coincides with the symmetry axis of the towing unit (see figure 1). Thus, $x^*_1(0) = 0$ and $\theta_l(0) = 0$, whereas $x^*_3(0) \cong \xi_M - (d + a_3)\theta_{lt}(0) = -(a_1 H_t + a_3)\theta_{lt} < 0$ (see Equation (5c), definition of H_t, and mind that θ_{lt} is constant in the steady turning). Going back in time along the circular path of P_1 as far as the position P_1' occupied when crossing the x axis, the correspondent time is $t' = -y_1(0)/v \cong -[a_1(1 + H_l + H_t) + a_3]/v$. As $\dot{x}_1 = u_l - v\theta_l - a_1\dot{\theta}_l$, where u_l and $\dot{\theta}_l$ are constant in steady conditions, one gets the abscissa x^*_1' of point P_1' and then the off-tracking $x^*_1' - x^*_3$ using the previous results:

$$\frac{x_1^{*\prime} - x^*_3}{a_1\delta} = (H_t + A_3)\frac{\theta_{lt}}{\delta} - \frac{U - \Omega}{V\delta}(1 + H_l + H_t + A_3) - \frac{\Omega}{2V\delta}(1 + H_l + H_t + A_3)^2 \tag{22}$$

It is possible to choose if the ESP control must be applied or not depending on the acceptableness of the "natural" response without ESP ($M_{ESP} = 0$). On the other hand, either with or without ESP, that is when the system parameters give a response with $\rho/\rho_{id.} \cong 1$ in most of the speed range, the cornering stiffness of the trailer wheels may be adjusted by varying the factor g_3 in order that the off-tracking remains within prefixed limits, at least in the low velocity range.

An approximate calculation of the steering behaviour for $M_{ESP} = 0$ may be made neglecting the small drag terms containing c_0V^2 in the steady dynamical matrix D_{steady}. Omitting some algebra and assuming the mass centre of the trailer over its axle ($A_3 = 0$), one obtains.

$$\frac{\rho}{\rho_{id.}} \cong 1 + \frac{V^2}{2K_1K_2(1 + A_2)^2}(K_2A_2 - K_1) \tag{23}$$

$$\frac{x_1^{*\prime} - x^*_3}{a_1\delta} \cong \left\{ H_t\frac{(H_l + H_t - A_2)}{(1 + A_2)} + (1 + H_l + H_t) - \frac{(1 + H_l + H_t)^2}{2(1 + A_2)} - \frac{V^2}{2K_2(1 + A_2)^2}\left[1 + H_l + \mu H_t(1 + A_2)\frac{K_2}{K_3}\right]\right\}\frac{\rho_{id.}}{\rho} \tag{24}$$

If the centre of mass of the leading unit is centred between the axles 1 and 2, one has $A_2 = 1$, $F_{z2} = F_{z1}$ and $K_2 = K_1$ by Equation (12). Hence no over-steering or under-steering occurs according to Equation (23) and the ESP control system is not necessary. Moreover, also the off-tracking trend may be contained within prefixed limits by properly planning the cornering stiffness of the trailer wheels, i. e. the factor g_3, which is included in K_3. Actually, one may impose opposite values of the off-tracking $x^*_1' - x^*_3$ for $V = 0$ and for a certain velocity V_x, for example $V_x = 3$. Using then Equation (24) and

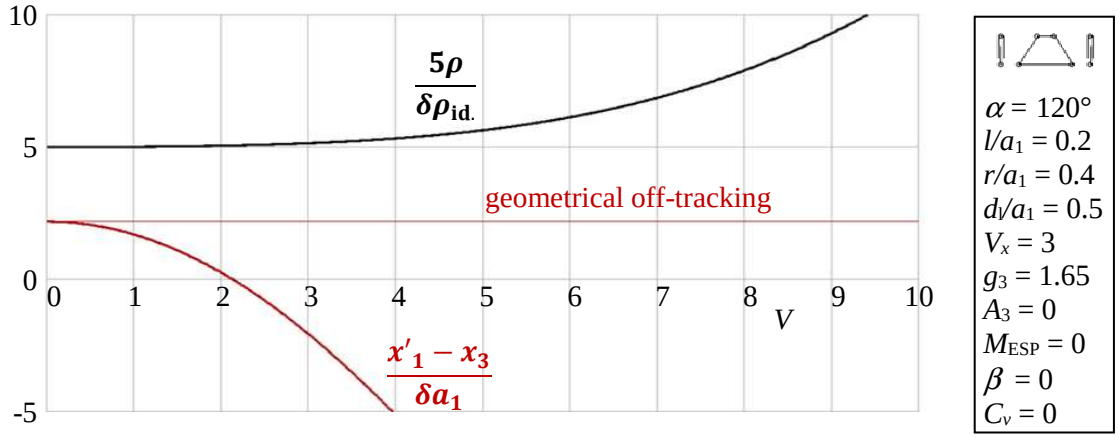

Figure 4. Four-bar linkage with forward converging bars. Radius of path curvature and off-tracking along road bend vs. vehicle speed after a steering command of the driver (δ).

solving for the ratio K_2/K_3, it is possible to calculate the needed value of the factor g_3. Of course, this result is acceptable if it yields feasible values for g_3.

It is interesting that the off-tracking limit for $V \to 0$, which characterizes its magnitude in the low velocity range, increases linearly with the distance H_t of the relative instant centre I from the trailer mass centre when the distance $H_l + H_t$ between the mass centres and A_2 are fixed. In this case, smaller off-tracking values are expected with backward converging bars in the low speed range.

Figure 4 shows the diagrams of the ratios $\rho/\rho_{id.}$ and $(x^*_1{}' - x^*_3)/(a_1\delta)$ for the case of figure 2. According to the above discussion, there is no need of electronic control of the steering conduct and the cornering stiffness of the trailer wheels is corrected so that the off-tracking of the range $0 < V < 3$ is not worse than the "geometrical" off-tracking for $V = 0$, where there is no cornering effect and all wheel paths are only affected only by the system geometry.

Figure 5 shows somewhat similar diagrams for the case of figure 3, where additional viscous dampers are present and the ESP system is such to cancel the difference $\rho/\rho_{id.} - 1$ altogether. The figure reports the dimensionless correcting moment M_{ESP} instead of $\rho/\rho_{id.}$. In this arrangement, the position of the third axle is a little ahead of the trailer mass centre ($A_3 = -0.15$), Equations (23-24) no longer apply and the results are obtained imposing that the moment M_{ESP} is such that the particular solution $\Omega/(V\delta) = 1/(1 + A_2)$ is obtainable by Equations (18), and then $\rho/\rho_{id.} = 1$ according to Equation (21b). Indicating with D_{2N} and D_{2M} the matrices obtainable replacing the second column of

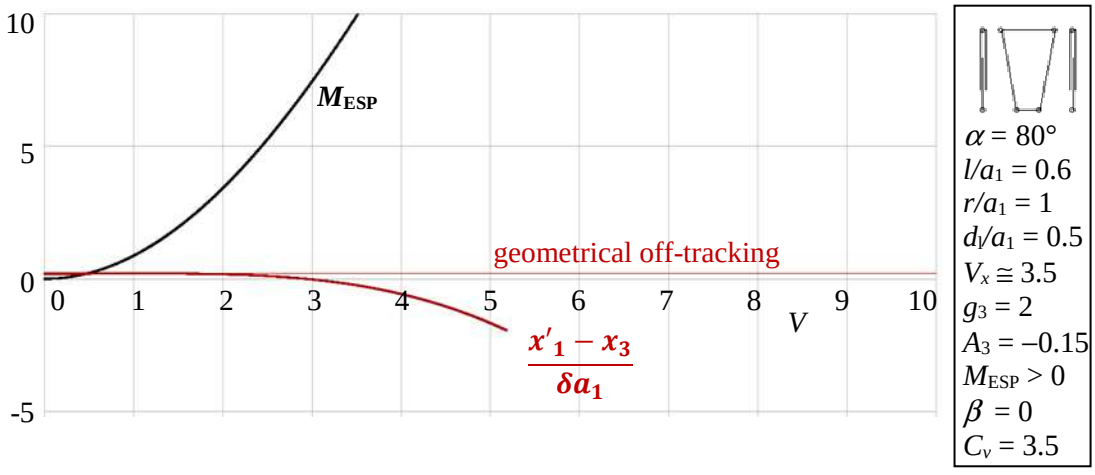

Figure 5. Four-bar linkage with backward converging bars. Correction moment by ESP system and off-tracking along road bend vs. vehicle speed after a steering command of the driver (δ).

D_{steady} with the column vectors $\{-1;\ 1 + H_l;\ H_t\}^T$ and $\{0;\ M_{ESP};\ 0\}^T$ respectively, one has $\Omega/(V\delta) = (2K_1/V)\ [\det(D_{2N}) + \det(D_{2M})]\ /\det(D_{steady})$. Hence, indicating with ρ the radius of curvature for $M_{ESP} = D_{2M} = 0$ and using Equation (21b), one has

$$M_{ESP} = \frac{\det(D_{steady})V}{2K_1(1+A_2)[D_{2M}(1,1) \times D_{2M}(3,3) - D_{2M}(1,3) \times D_{2M}(3,1)]}\left(1 - \frac{\rho_{id.}}{\rho}\right) \qquad (25)$$

Once M_{ESP} is calculated, the other variables U and θ_{vt} are obtained solving the complete system (18).

The off-tracking behaviour shown in figure 5 is very favourable and is achieved with small distances between the relative instant centre I and the trailer mass centre G_t, $H_t \cong 0.3$, and between the centre I and the third axle, $H_t + A_3 \cong 0.3 - 0.15 = 0.15$ (see data in the caption). It must be said that the off-tracking performances may worsen a little when changing these distances somehow, though they remain very good for $V \to 0$. Then, the configuration of figures 3 and 5 is feasible when there is good confidence that the load distribution on the trailer will remain unchanged during the journey and the mass centre will keep its position.

4. Conclusions

1) The stable or unstable behaviour of the articulated vehicles mainly depends on the vehicle speed and on the position of the semitrailer mass centre with respect to its axle. The lower speed values are generally stable but, on increasing the speed, an instable threshold is reached sooner or later.
2) The arrangement with forward converging drawbars is generally more stable than the backward converging one. Nevertheless, the stability may be improved at will by adding dampers in parallel to the traction bars.
3) The increase of the cornering stiffness of the third axle, i. e. of the semitrailer, generally enlarges the width of the stable region. The choice of the most convenient stiffness is correlated with the desired conditions as concerns the steering behaviour and the off-tracking along the bends.
4) Good stability and acceptable responses to the steering commands are obtainable by the forward converging bar linkages with no need of ESP correction and connecting dampers.
5) On the contrary, the backward converging bar linkages require ESP systems and dampers of the yaw motion, but permits achieving much better performances on the bends.

5. References

[1] Rajamani R 2006 *Vehicle Dynamic and Control* (Springer/Mechanical Engineering Series)
[2] Rocard Y 1954 *L'instabilité en Mécanique* (Paris: Masson et C.)
[3] Gillespie TD 1992 *Fundamental of Vehicle Dynamics* (SAE International)
[4] Pacejka HB 2006 *Tyre and Vehicle Dynamics* (Oxford: Butterworths-Heinemann)
[5] Fratila D and Darling J 1996 Simulation of coupled car and caravan handling behaviour *Vehicle System Dynamics* (*Int. J. of Vehicle Mechanics and Mobility* vol 26) pp 397-429
[6] Rossetter EJ and Gerdes JC 2002 A study of lateral vehicle control under a virtual force framework *Proc. of the 2002 Int. Symposium on Advanced Vehicle Control, Hiroshima, Japan.*
[7] Hac A, Fulk D and Chen H 2009 Stability and control considerations of vehicle-trailer combination *SAE Int. J. Passeng. Cars - Mech. Syst. 1(1)* pp 925-937
[8] Winkler CB 1986 Innovative Dollies: Improving the Dynamic Performances of Multi-Trailer Vehicles *1st Intern. Symposium on Heavy Vehicle Weights and Dimensions, Kelowna, Canada*
[9] Hensley Hitch, Hensley Mfg., Inc., http//hensleymfg.com/.
[10] Sorge F 2015 On the sway stability improvement of car-caravan systems by articulated connections *Vehicle system Dynamics* (*Intern. Jour. of Vehicle Mechanics and Mobility* vol 53-9) pp 1349-1372